

Interference between dissociating states in H_2O_2 and HOCl causes orientation of OH diatomic products

Andrew J. Alexander*

School of Chemistry, University of Edinburgh, West Mains Road, Edinburgh EH9 3JJ, United Kingdom

(Received 4 June 2002; published 26 December 2002)

H_2O_2 and HOCl were dissociated using circularly polarized light at wavelengths 330–370 nm, and angular-momentum polarization of OH ($^2\Pi$) products was measured using laser induced fluorescence. The OH ($J=0.5$) products exhibit orientation of angular momenta resulting from interference between excited dissociating states of the parent molecules.

DOI: 10.1103/PhysRevA.66.060702

PACS number(s): 33.80.Gj, 34.50.Gb, 82.50.Hp

Measurements of the directionality (polarization) of photofragment angular momenta have been used extensively as a means to understanding processes whereby molecules fall apart under irradiation. In particular, interference between multiple dissociative states produces distinct contributions (such as helicity) to the photofragment polarization, which allows the measurement of the phase differences of the asymptotic wave functions, and hence, the overall shapes of the participating dissociative surfaces [1–3]: the ultimate goal of molecular dynamics. However, studies of photofragment interference effects so far have been limited to measurement of polarization of atomic photofragments resulting from dissociation of diatomic [1,2,4–7] or triatomic species [8–10]. For example, Rakitzis *et al.* measured electronic orientation of Cl ($^2P_{3/2}$) atoms from the photodissociation of iodine monochloride (ICl) [6]. They found that the helicity of the orientation oscillated several times as a function of the wavelength of the dissociating light. Rotational orientation of diatomic photofragments resulting from dissociation of triatomic molecules has also been demonstrated [11,12]. Hasselbrink *et al.* studied the dissociation of ICN at 248 nm using circularly polarized photolysis radiation [11]. The helicity of the orientation of the diatomic fragments was found to oscillate as a function of the CN rotational angular momentum (N). More remarkably, the magnitude of the orientation was found to be $\langle N_z \rangle = -7.2 \pm 0.7$ in the range $39 \leq N \leq 55$. This magnitude of orientation is considerably larger than the photon angular momentum, or the electronic angular momentum of the fragments. Vigué *et al.* developed a model for the dissociation, based on amplification of the rotational angular momentum as a result of coherence between bending states of the ICN parent molecule [13]. By contrast, recent studies of the dissociation of NO_2 have also measured orientation of the NO diatomic photofragments [14]. In this case, the orientation does not result from interference between dissociating states, but is consistent with a classical model in which the departing O atom applies a torque to the N end of the NO molecule.

In this paper, we report the measurements of orientation of diatomic OH ($^2\Pi$) photofragments, resulting from interference between multiple electronic states of the dissociating

parent molecule at room temperature (298 K). The results are directly comparable to the observation of atomic Cl ($^2P_{1/2}$) orientation following photodissociation of Cl_2 [9]. Remarkably, however, the orientation of OH appears to survive thermal averaging of internal motions (e.g., torsion or bending) of the parent molecule, and the implicit averaging over multiple pathways across the potential-energy landscape of the molecule, resulting from the increased number of degrees of freedom of the system. Interference between the dissociating electronic states are observed without the need of an unusual amplification mechanism, making the results more general than previously recognized [11,13].

The experimental methodology followed is very similar to that described elsewhere [11]. Hydrogen peroxide solution (60% w/v) was distilled under vacuum, and then flowed through a polytetrafluoroethylene (PTFE) coated stainless steel vessel at total pressures < 100 mTorr. HOCl was produced by passing Cl_2 gas through a bed of glass beads coated with soda-ash moistened in water. Tunable photolysis radiation (330–370 nm) and probe radiation (~ 308 nm) for laser induced fluorescence (LIF) were produced by second-harmonic generation of the output of $\text{Nd}^{3+}:\text{YAG}$ (yttrium aluminum garnet)-pumped dye lasers. Both laser beams were circularly polarized using zero-order quartz quarter waveplates. The probe radiation was switched between left and right circularly polarized light on a shot-by-shot basis with a photoelastic modulator. The photolysis and probe laser beams were counter-propagated collinearly [11]. Doppler-resolved profiles $D(\nu)$ were obtained by scanning over individual rotational lines in the (0,0) band of the OH ($A-X$) electronic transition, and collecting the fluorescence without polarization analysis.

Tensor moments of the angular-momentum distribution in the laboratory frame $A_q^{(k)}$ were extracted from LIF intensities using the formalism developed by Kummel, Sitz, and Zare [15,16]. The LIF signal intensity can be written

$$D(\theta, \phi) = C(\det)n(J)[A_0^{(0)}(\theta, \phi) + P_0^{(1)}A_0^{(1)}(\theta, \phi)], \quad (1)$$

where $C(\det)$ is an undetermined constant function of the detection apparatus, $n(J)$ is the population of the rotational state J , and $P_0^{(1)}$ is the sensitivity of LIF to the $A_0^{(1)}$ [16]. The angular variables (θ, ϕ) are the angular coordinates of the parent molecule frame in the laboratory frame with the z axis defined by the photofragment velocity \mathbf{v} [17]. $A_0^{(0)}$ is propor-

*Electronic address: andrew.alexander@ed.ac.uk

tional to the differential cross section of the scattered photo-fragments, parameterized by β

$$4\pi A_0^{(0)}(\theta, \phi) = 1 + \beta P_2(\cos \theta), \quad (2)$$

where $P_2(\cos \theta)$ is the second Legendre polynomial. Similarly, orientation of angular momentum in the laboratory frame $A_0^{(1)}$ can be parameterized by molecule frame parameters $\mathbf{a}_q^{(k)}(p)$ [18]

$$4\pi A_0^{(1)}(\theta, \phi) = (1 + \beta) \mathbf{a}_0^{(1)}(\perp) \cos^2 \theta + \frac{1}{2} \mathbf{a}_{1+}^{(1)}(\parallel, \perp) \sin^2 \theta. \quad (3)$$

The Hertel-Stoll definitions of real spherical tensor moments have been used, $\mathbf{a}_{1+}^{(1)} = -\sqrt{2} \text{Re}[\mathbf{a}_1^{(1)}]$. The $\mathbf{a}_0^{(1)}$ represents orientation of \mathbf{J} along \mathbf{v} as a result of incoherent excitation of perpendicular (\perp) electronic transitions of the parent molecule

$$\mathbf{a}_0^{(1)}(\perp) = \langle J_z \rangle = \sum_{m_j} \frac{p(m_j) m_j}{\sqrt{J(J+1)}}, \quad (4)$$

where $p(m_j)$ is the probability of populating the state m_j , and m_j lies in the range $-J$ to $+J$. The $\mathbf{a}_{1+}^{(1)}(\parallel, \perp) = \langle J_x \rangle$ represents orientation of \mathbf{J} perpendicular to \mathbf{v} resulting from interference between parallel (\parallel) and perpendicular (\perp) transitions [18], and lies in the same range as $\mathbf{a}_0^{(1)}(\perp)$. At photolysis wavelengths around 355 nm, both H_2O_2 and HOCl exhibit mixed transitions. These are believed to be the $\bar{A}^1A(\perp)$ and the $\bar{B}^1B(\parallel)$ states of H_2O_2 , and the $1^1A''(\perp)$ and $1^3A''/2^1A'(\parallel)$ states of HOCl [19–21].

Monte Carlo simulations of Doppler contours $D(\nu)$ were obtained by one-dimensional projection of Eq. (1) onto the Doppler axis (i.e., the probe-laser propagation direction) and integrating contributions that shared the same projection on this axis. The sensitivity parameter $P_0^{(1)}$ changes sign according to the helicity (L/R) of the circularly polarized probe light. It is convenient to form composite sum and difference profiles $D_{\text{iso}}(\nu) = D_L(\nu) + D_R(\nu)$, and $D_{\text{aniso}}(\nu) = D_L(\nu) - D_R(\nu)$ [22]. $D_{\text{aniso}}(\nu)$ depends only on product orientation. $D_{\text{iso}}(\nu)$ includes both isotropic and alignment contributions to the angular-momentum polarization. We estimate the effects of alignment on $D_{\text{iso}}(\nu)$ for OH ($J=5.5$) to be small ($<2\%$) [23]. For OH ($J=0.5$) there can be no higher parameters $\mathbf{a}_q^{(k)}(p)$ with $k > 1$, i.e., the molecules can be *oriented*, but not *aligned* [15].

Experimental composite Doppler contours were fitted by nonlinear least-squares methods using basis sets of simulated contours with known $\mathbf{a}_q^{(k)}(p)$ [18]. Difference composite profiles resulting from H_2O_2 dissociation at 355 nm are shown in Fig. 1, comparing OH ($J=5.5$) and OH ($J=0.5$) products. The OH ($J=5.5$) results show incoherent orientation $\mathbf{a}_0^{(1)}(\perp) = 0.077 \pm 0.020$ in the molecular frame. By taking the ratio of integrated profiles we obtain

$$\frac{\langle D_{\text{aniso}} \rangle}{\langle D_{\text{iso}} \rangle} = \frac{P_0^{(1)}}{3} [(1 + \beta) \mathbf{a}_0^{(1)}(\perp) + \mathbf{a}_{1+}^{(1)}(\parallel, \perp)]. \quad (5)$$

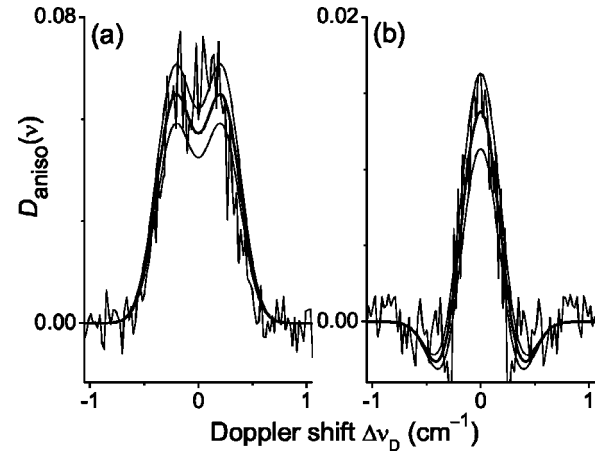


FIG. 1. Composite anisotropic Doppler profiles $D_{\text{aniso}}(\nu)$ (ragged line=experimental, thick solid line=best fitted model) for H_2O_2 dissociation at 355 nm [22]. The ordinate scales shown are relative to the respective $D_{\text{iso}}(\nu)$, which are normalized to unit area. (a) OH ($J=5.5$) via $P_{11}(N=5)$ LIF transition, best fit $\mathbf{a}_0^{(1)}(\perp) = 0.077$. (b) OH ($J=0.5$) via ${}^P Q_{12}(N=1)$ LIF transition, best fit $\mathbf{a}_0^{(1)}(\perp) = -0.046$, $\mathbf{a}_{1+}^{(1)}(\parallel, \perp) = 0.075$. Upper and lower thin solid lines represent simulations with best fit values ± 0.010 .

Using this equation, assuming that $\mathbf{a}_{1+}^{(1)}(\parallel, \perp) = 0$, we obtain $\mathbf{a}_0^{(1)} = 0.071 \pm 0.013$ for OH ($J=5.5$), in good agreement with the value obtained from fitting; we see no evidence for $\mathbf{a}_{1+}^{(1)}(\parallel, \perp)$ within the limits of our signal to noise. This result may be simply due to our inability to measure a small interference polarization effect over the background of a larger incoherent polarization effect. Some care must be taken over the interpretation of the molecular frame parameters $\mathbf{a}_q^{(k)}(\parallel, \perp)$. The electronic transition moment may not be exactly parallel or perpendicular to the direction of the lysing bond, and can be observed from incoherent transitions of either symmetry without interference. For example, if a linear triatomic happens to be excited during bending vibration, an observed $\mathbf{a}_{1+}^{(1)}(\parallel, \perp)$ may originate from parallel and perpendicular *projections* of an in-plane transition moment, as discussed by Ahmed *et al.* [8] for NO_2 dissociation, and by Kim *et al.* [7] in the case of OCS dissociation. For the H_2O_2 molecule, the bending mechanism would involve the symmetric (ν_2) and antisymmetric (ν_6) bends, and these are believed to cause the strong alignment $\mathbf{a}_{2+}^{(2)}(\perp) = 0.18 \pm 0.08$ observed for OH ($J=5.5$) [23]. Thus, it would appear that the OH ($J=5.5$) molecules exhibit alignment out of the molecular (yz) plane, but not orientation. In terms of the ν_2, ν_6 bending mechanism, there are as many OH bonds bending clockwise as are bending counterclockwise. It would seem reasonable that the circularly polarized photon has no selectivity over nuclear motion. On the other hand, the existence of some orientation in the molecular frame is expected in order to conserve the helicity of the whole system (circularly polarized photon + H_2O_2 molecule). Evidently, the observed $\mathbf{a}_0^{(1)}(\perp)$ is very much smaller than if J were maximally oriented parallel to velocity [if $m_j = J = 5.5$, $\mathbf{a}_0^{(1)}(\perp) = 0.920$]. We believe that the observed orientation is mainly due to the electronic part ($\Omega = 1.5$) of the total angular momentum J

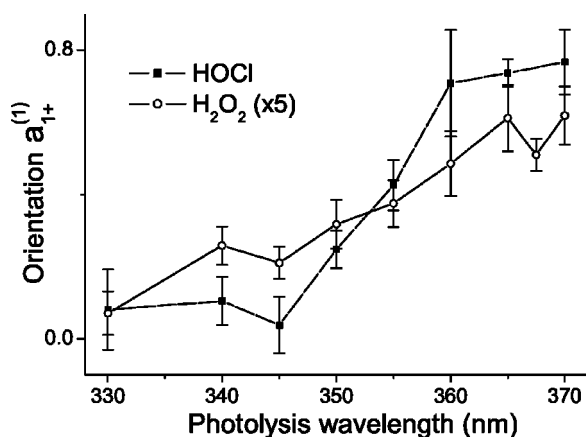


FIG. 2. Orientation parameter $\mathbf{a}_{1+}^{(1)}(\parallel, \perp)$ for OH ($J=0.5$) as a function of photolysis wavelength for H_2O_2 dissociation (empty circles, solid line) and for HOCl dissociation (solid squares, dashed line) [22]. The H_2O_2 data have been multiplied by a factor of 5 in order to plot them on the same scale.

=5.5: this seems reasonable since it is the electrons that are primarily excited by the photolysis radiation. If we assume that the angular momentum ($1\hbar$) of the circularly polarized photon is shared between the OH molecules, we give $m_J = 1/2$ to each fragment, to estimate an orientation $\mathbf{a}_0^{(1)}(\perp) = 1/[2\sqrt{J(J+1)}] = 0.084$: very close to the experimental result. Certainly, we see no evidence for amplification of angular momentum, or rather, we see no evidence of amplification of the *helicity* of angular momentum.

For OH ($J=0.5$) products from H_2O_2 dissociation at 355 nm, we observe both $\mathbf{a}_{1+}^{(1)}(\parallel, \perp) = 0.075 \pm 0.032$ and $\mathbf{a}_0^{(1)}(\perp) = -0.046 \pm 0.019$. The observed parameters are smaller than maximal [for $J=0.5$, maximal $\mathbf{a}_q^{(1)}(p) = 0.577$]. The $\mathbf{a}_0^{(1)}(\perp)$ is of similar magnitude to that for OH ($J=5.5$). The fact that we do not observe an $\mathbf{a}_{1+}^{(1)}(\parallel, \perp)$ for OH ($J=5.5$) fragments may be due to averaging as a result of the larger rotational motion ($N=5$) of the OH ($J=5.5$) molecules, which are known to have a strong torsional motion due to the shape of the dissociating potential-energy surfaces [19]. For racemic H_2O_2 the torsional dissociation is achiral, and cannot enhance the orientation. Torsional motion around the dissociating O–O causes the OH molecules to rotate away from the HO–OH moleculelike propeller blades (\mathbf{J} aligned parallel to \mathbf{v}) and would average out electronic orientation with respect to the molecule (yz) plane, i.e., $\mathbf{a}_{1+}^{(1)}(\parallel, \perp) \approx 0$. Alternatively, a measurement of $\mathbf{a}_{1+}^{(1)}(\parallel, \perp) \approx 0$ may result from a coincidental near-zero asymptotic phase difference between \parallel and \perp states at this dissociation energy (355 nm).

In an attempt to address the question of whether the observed $\mathbf{a}_{1+}^{(1)}(\parallel, \perp)$ for $J=0.5$ involves interference between multiple electronic states or simply coherence from bending of a single state, we measured the $\mathbf{a}_{1+}^{(1)}(\parallel, \perp)$ as a function of the photolysis wavelength for both the H_2O_2 molecule, and the HOCl molecule [24]. The results are shown in Fig. 2, and show an increase in the $\mathbf{a}_{1+}^{(1)}(\parallel, \perp)$ with increasing photolysis wavelength for both molecules. The $\mathbf{a}_{1+}^{(1)}(\parallel, \perp)$ are much smaller for the H_2O_2 molecule. This may be due to blurring

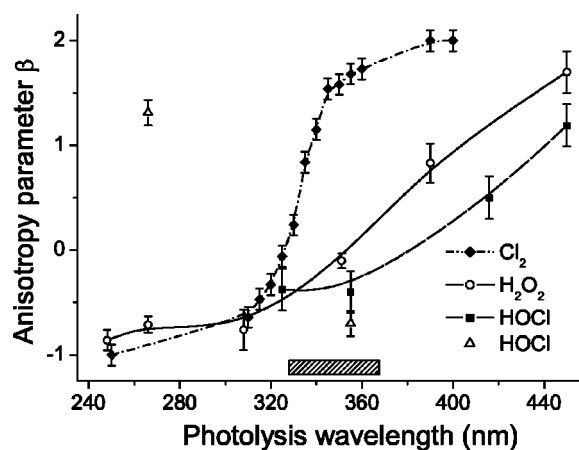


FIG. 3. OH translation anisotropy beta parameter β , as a function of photolysis wavelength for H_2O_2 (empty circles [19]), HOCl (empty triangles [26]), HOCl (filled squares [20]). Also shown are β for Cl^* (${}^2P_{1/2}$) atoms measured from Cl_2 dissociation (filled diamonds [27]). The shaded bar indicates the wavelength range of Fig. 2.

of the orientation caused by a spread in the OH partner fragment state for the H_2O_2 molecule. Theoretical quantum calculations suggest that the two OH radicals formed are nearly identical on average [25]. The monatomic Cl (2P_J) partner fragments of HOCl, on the other hand, greatly reduce the possible energy spread in the products.

Perhaps the most significant observation about Fig. 2 is that the $\mathbf{a}_{1+}^{(1)}(\parallel, \perp)$ appears to increase with increasing contribution of the parallel states. To further this point, we have plotted translational anisotropy (β) parameters for H_2O_2 , HOCl, and Cl_2 in Fig. 3, as a function of photolysis wavelength. Figure 3 shows that electronic states with parallel symmetry make an increasing contribution as the photolysis wavelength is tuned to longer wavelength. The similarity between the trends for H_2O_2 and HOCl in Figs. 2 and 3 is very striking. In terms of a model involving interference between parallel and perpendicular states, the energy dependence of $\mathbf{a}_{1+}^{(1)}(\parallel, \perp)$ is proportional to the cosine of the asymptotic phase difference ($\Delta\phi = \phi_{\perp} - \phi_{\parallel}$) between the radial parts of the outgoing wave functions from parallel and perpendicular transitions, and the amplitude is also modulated by the degree of mixing $\sqrt{(1+\beta)(2-\beta)}$ [9]. The fact that the $\mathbf{a}_{1+}^{(1)}(\parallel, \perp)$ appears to increase with the mixing of the parallel and perpendicular states supports our assertion that the effect that we have measured is interference born from fragments travelling via two different electronic states of different symmetry. It is also clear that the $\mathbf{a}_{1+}^{(1)}(\parallel, \perp)$ becomes almost zero as the transition becomes almost purely perpendicular for both H_2O_2 and HOCl. This would not be expected if the mechanism for producing the $\mathbf{a}_{1+}^{(1)}(\parallel, \perp)$ was the result of coherence due to bending motions of the parent molecule [7].

Finally, the results plotted in Fig. 2 are similar to those of the orientation parameter $\text{Im}[\mathbf{a}_{1+}^{(1)}(\parallel, \perp)] \propto \sin(\Delta\phi)$ measured for Cl^* (${}^2P_{1/2}$) fragments from Cl_2 photolysis by Kim *et al.*

[9]. The measurements of β , and of $\mathbf{a}_{1+}^{(1)}(\parallel, \perp)$, for Cl_2 , HOCl , and H_2O_2 all show remarkable similarities. We would expect that a much greater degree of averaging over product pathways would be required to model the present results. Despite the implicit averaging involved, the orientation due to interference does appear to survive in $\text{OH} (^2\Pi)$.

Clearly, these effects are general, and not limited to atomic products of simple diatomic species, as might first have been expected.

A.J.A. thanks the Royal Society for financial support and the EPSRC Central Laser Facility for the loan of a YAG and dye laser.

-
- [1] A.S. Bracker, E.R. Wouters, A.G. Suits, Y.T. Lee, and O.S. Vasutinskii, *Phys. Rev. Lett.* **80**, 1626 (1998).
- [2] O.S. Vasutinskii, *Faraday Discuss. Chem. Soc.* **113**, 77 (1999); K.O. Korovin, B.V. Picheyev, O.S. Vasutinskii, H. Valipour, and D. Zimmermann, *J. Chem. Phys.* **112**, 2059 (2000).
- [3] A.J. Alexander and R.N. Zare, *Acc. Chem. Res.* **33**, 199 (2000).
- [4] J. Vigué, P. Grangier, G. Roger, and A. Aspect, *J. Phys. (France) Lett.* **42**, L531 (1981).
- [5] T.P. Rakitzis, S.A. Kandel, and R.N. Zare, *J. Chem. Phys.* **108**, 8291 (1998).
- [6] T.P. Rakitzis, S.A. Kandel, A.J. Alexander, Z.H. Kim, and R.N. Zare, *Science* **281**, 1346 (1998); *J. Chem. Phys.* **110**, 3351 (1999).
- [7] Z.H. Kim, A.J. Alexander, and R.N. Zare, *J. Phys. Chem. A* **103**, 10 144 (1999).
- [8] M. Ahmed, D.S. Peterka, A.S. Bracker, O.S. Vasutinskii, and A.G. Suits, *J. Chem. Phys.* **110**, 4115 (1999).
- [9] Z.H. Kim, A.J. Alexander, S.A. Kandel, T.P. Rakitzis, and R.N. Zare, *Faraday Discuss. Chem. Soc.* **113**, 27 (1999).
- [10] T.P. Rakitzis, P.C. Samartzis, and T.N. Kitsopoulos, *Phys. Rev. Lett.* **87**, 123001 (2001).
- [11] E. Hasselbrink, J.R. Waldeck, and R.N. Zare, *Chem. Phys.* **126**, 191 (1988); R.N. Zare, *Faraday Discuss. Chem. Soc.* **84**, 180 (1987).
- [12] M.L. Costen and G.E. Hall, *Faraday Discuss. Chem. Soc.* **113**, 481 (1999).
- [13] J. Vigué, B. Girard, G. Gouédard, and N. Billy, *Phys. Rev. Lett.* **62**, 1358 (1989).
- [14] V.K. Nestorov and J.I. Cline, *J. Chem. Phys.* **111**, 5287 (1999); M. Brouard, P. O’Keeffe, D.M. Joseph, and D. Minayev, *Phys. Rev. Lett.* **86**, 2249 (2001).
- [15] R.N. Zare, *Angular Momentum* (Wiley, New York, 1988).
- [16] A.C. Kummel, G.O. Sitz, and R.N. Zare, *J. Chem. Phys.* **88**, 7357 (1988). Note that E_0^1 for case A in Table III of this paper should read $(1/\sqrt{2})\sin 2\beta$.
- [17] L.D.A. Siebbeles, M. Glass-Maujean, O.S. Vasutinskii, J.A. Beswick, and O. Rocero, *J. Chem. Phys.* **100**, 3610 (1994).
- [18] T.P. Rakitzis and R.N. Zare, *J. Chem. Phys.* **110**, 3341 (1999).
- [19] M. Brouard, M.T. Martinez, C.J. Milne, J.P. Simons, and J.-X. Wang, *Chem. Phys. Lett.* **165**, 423 (1990).
- [20] R.J. Barnes, A. Sinha, and H.A. Michelsen, *J. Phys. Chem. A* **102**, 8855 (1998).
- [21] S. Nanbu and S. Iwata, *J. Phys. Chem.* **96**, 2103 (1992).
- [22] The absolute sign of the parameters $\mathbf{a}_{q\pm}^{(1)}(p)$ were not determined because we did not determine the helicity of circular polarization used in the experiments.
- [23] A.J. Alexander, *J. Chem. Phys.* (to be published).
- [24] Unfortunately, constraints of our experimental apparatus did not allow us to make measurements at photolysis wavelengths greater than 370 nm.
- [25] Z.T. Cai, D.H. Zhang, and J.Z.H. Zhang, *J. Chem. Phys.* **100**, 5631 (1994).
- [26] H. Fujiwara and T. Ishiwata, *J. Phys. Chem. A* **102**, 3856 (1998).
- [27] P.C. Samartzis, B.L.G. Bakker, T.P. Rakitzis, D.H. Parker, and T.N. Kitsopoulos, *J. Chem. Phys.* **110**, 5201 (1999).